CHAOS
Theory and Applications
in Applied Sciences and Engineering

e-ISSN: 2687-4539
RESEARCH ARTICLE
Vol.6 / No.2 / 2024 / pp.83-89
Special Issue (EDIESCA 2023)
https://doi.org/10.51537/chaos.1376471

Analysis of the Dynamics of a ϕ^6 Duffing Type Jerk System

A. Bucio-Gutiérrez [α,1], **E. S. Tututi-Hernández** [α,2] **and U. Uriostegui-Legorreta** [α,3]
[α]Facultad de Ciencias Físico Matemáticas, UMSNH, Av. Francisco J. Múgica S/N, 58030, Morelia, Michoacán, México.

ABSTRACT

A theoretically and numerically analysis on Duffing Jerk systems with a sixth-order type potential and a sixth-order potential smoothed by a Gaussian function are carried out in this work. This kind of systems can modelate the response in circuits which may be used in cryptography. The Jerk system is transformed into a dynamical system of dimension three. Choosing the set of values for the parameters to guaranty that Jerk systems are Duffing type with triple well potential. The dynamics and stability of the resulting system are analyzed, through phase space, bifurcation diagrams and Lyapunov exponents by varying the relevant parameters, finding the existence of a strange attractor. The dynamics of system with potential smoothed was studied by varying the smoothing parameter α, finding that this parameter can be used to controlling chaos, since the exponential factor keeps the same fixed points and it regulates smoothly the amplitude of the potential.

KEYWORDS

Jerk system
Duffing system
Bifurcation diagrams
Lyapunov exponent

INTRODUCTION

In recent years, Jerk systems have been the subject of great interest in the specialized community (Louodop *et al.* 2017; Kengne *et al.* 2020). In fact, the wide range of applications in fields such as control engineering (Raineri and Bianco 2019), biomechanics (Sharker *et al.* 2019) and robotics (Chen and Zhang 2016) in which it is necessary a third order derivative for the description of the system. This type of systems are, in general, described by the following equation

$$\dddot{x} = J\left(\ddot{x}, \dot{x}, x\right), \tag{1}$$

where the J stands for "Jerk" (Louodop *et al.* 2017), which represents a measure of the "abruptness" or "smoothness" of movement (from a classical perspective).

Jerk systems can describe phenomena and behaviors more complex than traditional second-order systems, which makes them useful in modeling and controlling systems that experience rapid changes or nonlinearities. Among the Jerk systems the most notable are those that present chaotic behavior. In an autonomous Jerk system, this chaotic behavior is achieved by considering a certain degree of nonlinearity in J and because an increase in this nonlinearity does not necessarily lead to a greater degree of chaos in the system (Patidar and Sud 2005). However, it is possible to work with systems with subjectively simple nonlinearities.

In physical models, Jerk-type arrangements can be used to model, for example, the Nosé-Hoover dynamic system in thermostated dynamic which exhibits time-reversible Hamiltonian chaos (Posch *et al.* 1986). Furthermore, Jerk systems are often implemented in variants of circuits, as they are easy to analyze numerically and experimentally, and can be easily scaled to a wide range of frequencies (Sprott 2011), with hump structure (Folifack Signing *et al.* 2021) and a memristive model with quadratic memductance which is used to build the nonlinear term of a Jerk system (Njitacke *et al.* 2022). Those Jerk systems are used to image encryption.

Due to its applicability in modeling synchronization, one of the most recurring system in the literature on chaos is the non-linear Duffing oscillator (Uriostegui-Legorreta and Tututi-Hernández 2022; Uriostegui and Tututi 2023). Although the Duffing oscillator is a dynamical system of low dimensionality, it can present chaos if it is under an external forcing. Moreover, chaotification (Zhang *et al.* 2009) allows converting the dynamics of autonomous systems to a non-periodic one that presents chaotic motion. Different control methods and chaotification techniques of discrete-time and

Manuscript received: 16 October 2023,
Revised: 25 November 2023,
Accepted: 1 December 2023.

[1]1207258b@umich.mx (**Corresponding author**)
[2]eduardo.tututi@umich.mx
[3]ulises.uriostegui@umich.mx

continuous-time dynamic systems exist in the literature, such as feedback control with temporal delay (Zhou *et al.* 2010) or the cosine chaotification technique (Natiq *et al.* 2019). Furthermore, the chaotic dynamics of the non-linear system can be modulated to obtain a stable state or different types of dynamics (Haluszczynski and Räth 2021)

However, in the first instance it is necessary to identify under what parameters or conditions the system presents a chaotic behavior. For this purpose, it is necessary to find regions of the parameters space that present non-periodical behavior. Thus, methods such as bifurcation diagrams and Lyapunov's spectrum, constituted by Lyapunov's characteristic exponents (LCE), result useful. In last case, a positive LCE is indicative of the presence of a chaotic attractor in the system (Sandri 1996).

In this work, we study both a Duffing Jerk system with sixth-order potential and a Duffing Jerk system with sixth-order potential smoothed by a Gaussian function. The proposed systems are analyzed numerically, showing a change in dynamics by changing the smoothed factor that ranges from presenting chaos to presenting a limit cycle. In addition, we classify the dynamics of the system for different parameters finding that an increase in the smoothed factor leads to restricting the dynamics to two types.

THEORETICAL FRAMEWORK

System

The dynamics of the Jerk system with a potential type ϕ^6 is given by

$$\dddot{x} = -c_1\ddot{x} - c_5c_2\dot{x} + c_5\frac{d}{dx}U(x), \tag{2}$$

being

$$U(x) = \frac{x^2}{2} + \frac{c_3x^4}{4} + \frac{c_4x^6}{6}, \tag{3}$$

the energy potential. Whenever $c_4 > 0$ and $c_3 < 0$, U is triple well potential (Hong *et al.* 2015; Uriostegui-Legorreta and Tututi 2023a,b). Notice that Eq.(2) can be written as an autonomous dynamical system, as follows

$$\begin{aligned}\dot{x} &= y,\\ \dot{y} &= c_5z,\\ \dot{z} &= -c_1z - c_2y + \frac{d}{dx}U(x),\end{aligned} \tag{4}$$

where the c_1, c_2, c_3, c_4 and c_5 parameters are real numbers. Since the system in Eq.(4) is nonlinear and three-dimensional, it could give rise to chaos. In the following it will be established the conditions for chaos.

It is well known that there exists an attractor if the ratio of the contraction of the volume (V) of initial conditions in phase space over time is less than zero(Hilborn *et al.* 2000), that is

$$\frac{1}{V}\frac{dV}{dt} = \frac{\partial\dot{x}}{\partial x} + \frac{\partial\dot{y}}{\partial y} + \frac{\partial\dot{x}}{\partial z} = -c_1 < 0, \tag{5}$$

which is satisfied for $c_1 > 0$. It is known that when $\frac{1}{V}\frac{dV}{dt} < 0$, the volume contracts exponentially thus the system results dissipative and there may be a stable attractor. On the other hand, when $\frac{1}{V}\frac{dV}{dt} > 0$ the volume in phase space expands and there are only unstable fixed points, limit cycles or chaotic repellers; that is, the dynamics diverge if the initial condition is not exactly one of the fixed points. These points (x_0, y_0, z_0) are given by

$$\begin{aligned}\frac{d}{dx}U(x)\,|_{x_0} &= 0,\\ y_0 &= 0,\\ z_0 &= 0.\end{aligned} \tag{6}$$

Hence, the fixed points depend on the parameters of $U(x)$.

To analyze the dynamics, it is necessary obtain the eigenvalues of the Jacobian matrix J of the system, given by

$$J = \begin{pmatrix} 0 & 1 & 0\\ 0 & 0 & c_5\\ \mu(x) & -c_2 & -c_1\end{pmatrix}, \tag{7}$$

with

$$\mu(x) = 1 + 3c_3x^2 + 5c_4x^4. \tag{8}$$

Notice that Eq. (8) is the second derivative with respect to x of the Eq. (3). In this manner, the characteristic polynomial evaluated at each of the fixed points is

$$P(\lambda) = -\lambda^3 - c_1\lambda^2 - c_2c_5\lambda - c_5\mu(x_0), \tag{9}$$

from which, we obtain the type of stability of the fixed points. Notice that Eq. (9) gives three solutions λ_1, λ_2, and λ_3, for which, the dynamics of the system depends on these values. The classification of the stability of system is shown in Table 1 (Francomano *et al.* 2017; Stumpf *et al.* 2011) .

Potential Function $U(x)$

Notice that $\frac{d}{dx}U(x)$ can be written as

$$\frac{d}{dx}U(x) = (x-0)(x-p^+)(x+p^+)(x-p^-)(x+p^-), \tag{10}$$

being

$$p^{\pm}(c_3, c_4) = \pm\sqrt{\frac{1}{2c_4}\left(-c_3 \pm \sqrt{c_3^2 - 4c_4}\right)}, \tag{11}$$

consequently, the fixed points of the system in Eq. (4) are

$$\begin{aligned}x_0 &= 0, p^+, -p^+, p^-, -p^-,\\ y_0 &= 0,\\ z_0 &= 0.\end{aligned} \tag{12}$$

The $p^{\pm}(c_3, c_4)$ in Eq. (11) are, in general, complex functions, so different scenarios can occur: i) all roots are real, ii) one root is real and 4 complex roots (2 complex and its conjugated), iii) 3 real roots and 2 complex roots (1 complex root an its conjugated). It is assume that all the roots are different, otherwise a degenerate case is obtained which is avoided for the interest of the problem.

Then, the conditions for Eq. (11) to be purely real are

$$c_4 \leq \left(\frac{c_3}{2}\right)^2 \tag{13}$$

and

$$\frac{1}{2c_4}\left(-c_3 \pm \sqrt{c_3^2 - 4c_4}\right) \geq 0. \tag{14}$$

In the case of the triple well potential, only the condition in Eq. (13) is necessary. The first condition is bounded by the upper parabola

Table 1 Classification of equilibrium points for 3D system with two complex eigenvalues and one real λ_1.

Equilibrium type	Relation
Asymptotically Stable Focus-Node	$\mathrm{Re}(\lambda_1) < \mathrm{Re}(\lambda_2) = \mathrm{Re}(\lambda_3) < 0$ $\mathrm{Im}(\lambda_2) = -\mathrm{Im}(\lambda_3)$
Unstable Focus-Node	$0 < \mathrm{Re}(\lambda_1) < \mathrm{Re}(\lambda_2) = \mathrm{Re}(\lambda_3)$ $\mathrm{Im}(\lambda_2) = -\mathrm{Im}(\lambda_3)$
Repelling Focus-Saddle	$\mathrm{Re}(\lambda_1) < 0 < \mathrm{Re}(\lambda_2) = \mathrm{Re}(\lambda_3)$ $\mathrm{Im}(\lambda_2) = -\mathrm{Im}(\lambda_3)$
Attracting Focus-Saddle	$\mathrm{Re}(\lambda_3) = \mathrm{Re}(\lambda_2) < 0 < \mathrm{Re}(\lambda_1)$ $\mathrm{Im}(\lambda_3) = -\mathrm{Im}(\lambda_2)$

defined by $c_4 = (c_3/2)^2 : c_3 \in \{-\infty, \infty\} \,/\, \{0\}$. However, it must satisfy at the same time with the second condition, so two cases occur. The first one being with the positive root

$$p^+ \begin{cases} c_4 \leq \left(\frac{c_3}{2}\right)^2, \\ \frac{c_3}{c_4} \leq \frac{\sqrt{c_3^2 - 4c_4}}{c_4}. \end{cases} \tag{15}$$

The region where it is purely real is found graphically by looking at the regions where the imaginary part of p^+ is zero as shown in Figure 1 (a). In the same way, in the second case with the negative root should occur that the imaginary part of p^- must be zero as shown the Figure 1 (b) in te regions delimited by

$$p^- \begin{cases} c_4 \leq \left(\frac{c_3}{2}\right)^2, \\ \frac{c_3}{c_4} \geq -\frac{\sqrt{c_3^2 - 4c_4}}{c_4}. \end{cases} \tag{16}$$

Figures 1 (a) and (b) show the region where $p^{\pm}$ are pure real. That is for $c_3 < 0$, $c_4 > 0$ and $c_4 < (c_3/2)^2$. In the subsequent discussion it is restricted to the case of the triple well potential.

NUMERICAL ANALYSIS

Bifurcation Diagrams

In order to obtain a dissipative system, it is necessary to take $c_5 > 0$ and $c_2 > 0$ (Louodop *et al.* 2014). To obtain the bifurcation diagrams as function of the c_1, c_2 and c_5 and identify the chaotic regions of the system, we take the values $c_3 = -0.6$ and $c_4 = 0.06$ and take two different initial conditions $\mathbf{x}_1 = (2.7083, 0, 0)$ and $\mathbf{x}_2 = (-2.7083, 0, 0)$, being $\mathbf{x}_i = (x_i, y_i, z_i)$ with $i = 1, 2$, both taken at the same initial time $t = 0$. In Figure 2 it is shown the bifurcation diagrams for the two initial conditions. These bifurcation diagrams were obtained by considering the local maxima of $x(t)$, $y(t)$ and $z(t)$ as a function of the c_1, c_2 and c_5 parameters, respectively, in a interval of time between $[250, 310]$, using a step time of 0.01 in the fourth-order Runge–Kutta method.

Phase Space

As it can be observed from Figure 2 there are regions where the system exhibits chaos. A particular set of values of the parameters

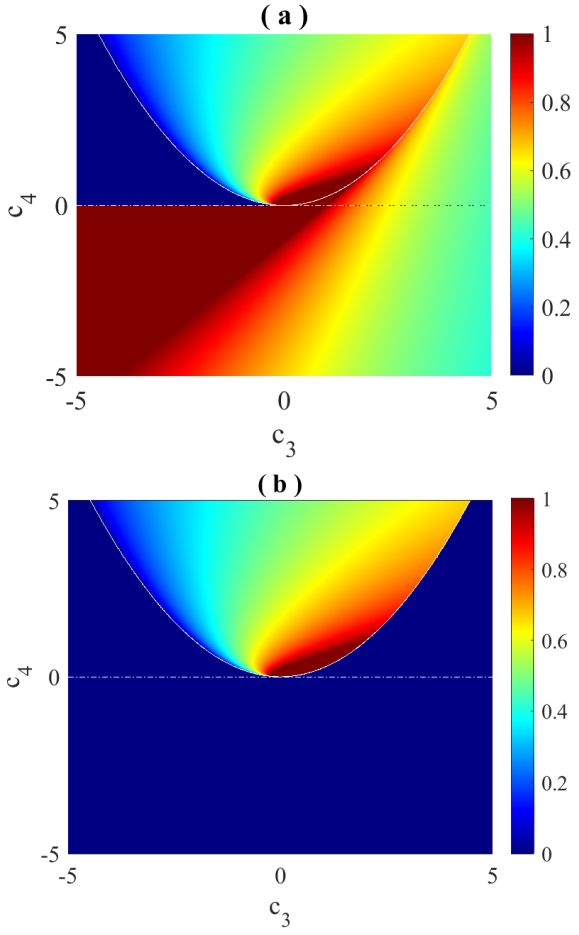

Figure 1 Values of imaginary part of p^+ in (a) and p^- in (b), both normalized to its maximum value.

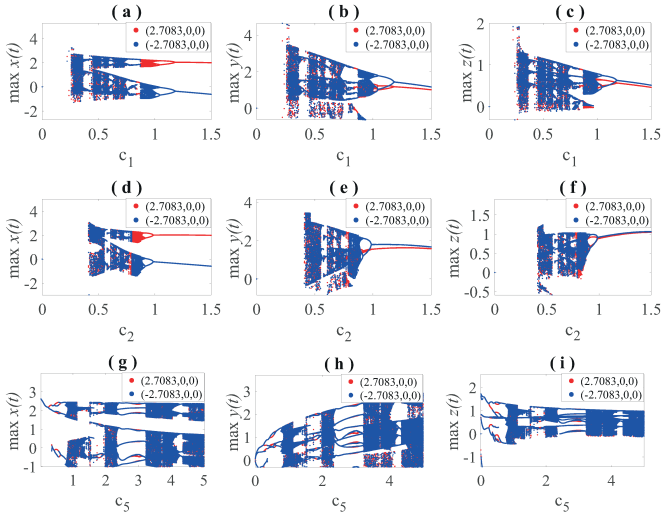

Figure 2 Bifurcation diagrams for the initial conditions $\mathbf{x}_1 = (2.7083, 0, 0)$ in red and $\mathbf{x}_2 = (-2.7083, 0, 0)$ in blue, as function the parameters. The first column (Figures (a), (d) and (g)) is for the x variable. The second column (Figures (b), (e) and (i)) is for the y variable, and finally the third column is for the z variable.

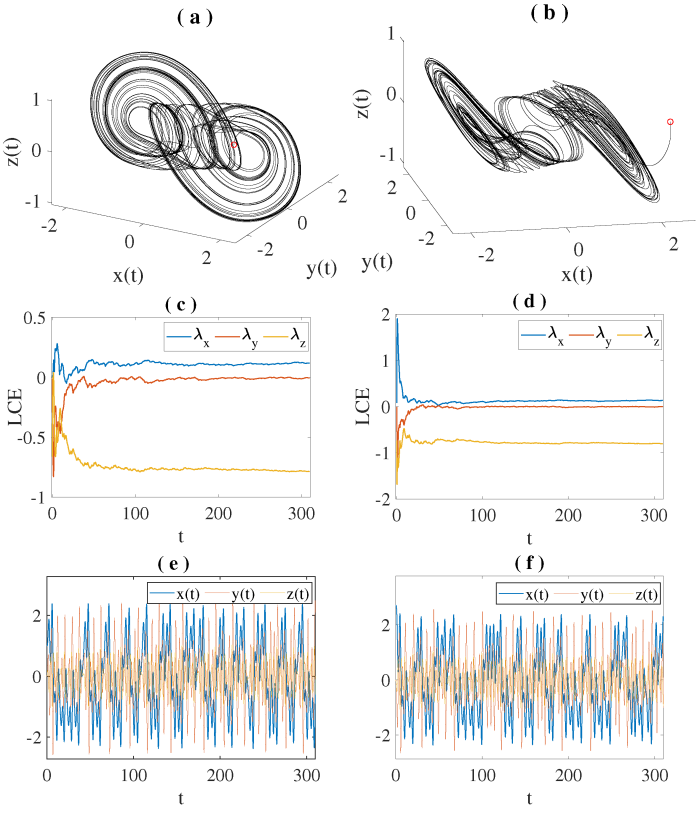

Figure 3 The strange attractors for the Jerk system obtained for the initial conditions of $(1, 0, 0)$ (a) and $(2.7083, 0, 0)$ (b). In (c) and (d) it is displayed the Lyapunov exponents for the corresponding initial conditions. In (e) and (f) it is shown the corresponding time series for the variables x, y and z.

is

$$\begin{aligned} c_1 &= 0.67, \\ c_2 &= 0.7, \\ c_3 &= -0.6, \\ c_4 &= 0.06, \\ c_5 &= 3.55, \end{aligned}$$

which are used for obtain the attractor solutions, shown in figure Figure 3 (a) and (b). The fixed points in Eq. (12) are found by substituting the respective parameters into Eq. (11), resulting the values $x_0 = 0, 2.8083, -1.4537, -2.8083, 1.4537$ with $y_0 = z_0 = 0$. We are interested in corroborating that the solutions obtained with the values of the parameters correspond to strange attractors. To do that it is necessary to obtain the LCE. According to reference (Wolf *et al.* 1985), for a 3-dimensional system, where it is possible to define tree Lyapunov exponents, if one Lyapunov exponent is positive, other equal to zero and the third is negative then it is obtained a strange attractor. It will be used this criterion for the following analysis. In Figures 3 (a) and (b) it is displayed the attractor obtained for the initial conditions of $(1, 0, 0)$ (a) and $(2.7083, 0, 0)$ (b). In Figures 3 (c) and (d) it is shown the Lyapunov exponent for these initial conditions, respectively. The values LCEs, at the time $t = 310$, obtained are $0.1193, -0.0040, -0.7853$ for the first initial condition and $0.1329, -0.0016, -0.8013$ for the second initial condition. Figures 3 (e) and (f) show the time series for the the variables x, y and z in a time interval of $[0, 310]$. As it can be observed the results are not periodic. According to (Wolf *et al.* 1985) the results indicates the presence of strange attractors.

Adding smoothed

Now let us add an exponential term that smooths the derivative of the potential in the system under study, hence the new system is

$$\begin{aligned} \dot{x} &= y, \\ \dot{y} &= c_5 z, \\ \dot{z} &= -c_1 z - c_2 y + \left(\frac{d}{dx} U(x)\right) e^{-\alpha x^2}, \end{aligned} \tag{17}$$

where $\alpha \geq 0$ is the smoothing term. In the case of $\alpha = 0$ it is recovered the former system. Notice that its fixed points, Jacobian and characteristic polynomial of the system described by Eq. (17) do not change in its form, (see Eq.(7)) except for the function

$$\mu_\alpha(x) = \left[1 + (3c_3 - 2\alpha) x^2 + (5c_4 - 2\alpha c_3) x^4 - 2\alpha c_4 x^6\right] e^{-\alpha x^2}. \tag{18}$$

Defining the function

$$\phi_\alpha(x) = \left(\frac{d}{dx} U(x)\right) e^{-\alpha x^2}, \tag{19}$$

whose behavior is illustrated in Figure 4 for different values of α.

With the introduction of the smoothing term, it is possible to obtain bifurcation diagrams varying α in Eqs. (17) to recognize the chaotic regions of the smoothed system. In Figure 5 it is shown the bifurcation diagrams as a function of this parameter. As expected, for small values of α, the system remains chaotic, while for values greater than 0.1, the system becomes non-chaotic, since the nonlinear terms tends to zero for values of α large enough. Despite the presence of regions of non-periodic behavior in the bifurcation diagrams there is a transition to regions of periodicity in which it can be found limit cycles in a region of the parameter

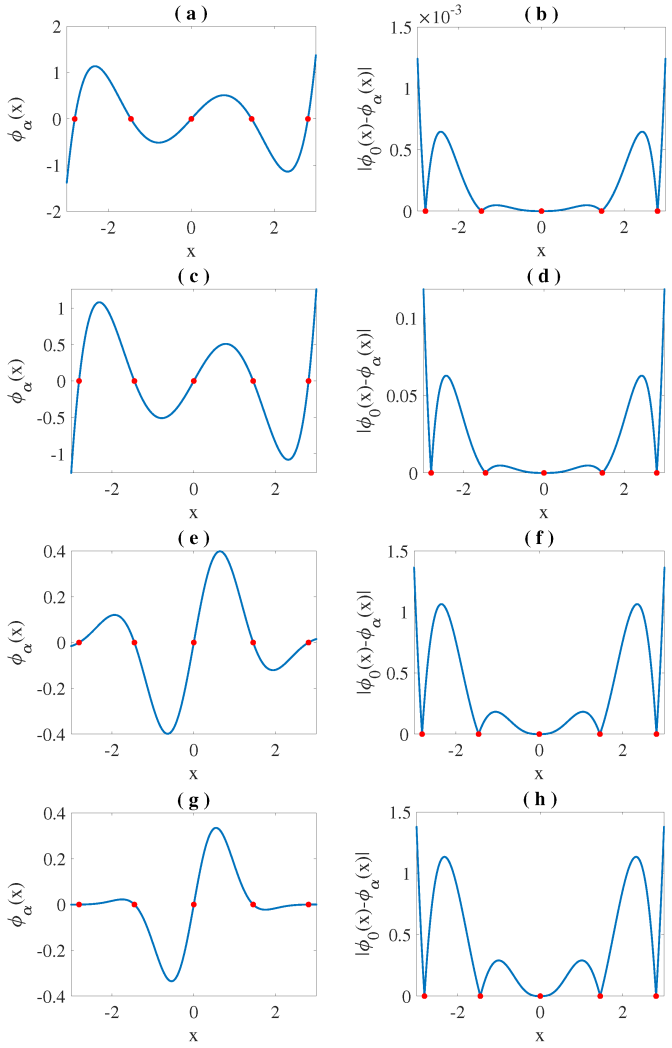

Figure 4 Functions $\phi_\alpha(x)$ (left) and $|\phi_0(x) - \phi_\alpha(x)|$ (right) for $\alpha = 1 \times 10^{-4}$, in (a), $\alpha = 1 \times 10^{-2}$ in (c), $\alpha = 0.5$ in (e) and $\alpha = 1$ in (g). Fixed points in red.

α. In fact, a qualitative analysis is carried out in the phase space of the trajectories at different values of α, finding a limit cycle for a value of $\alpha = 0.5$. This assertion is verified with the values of the LCE obtained for this case $\lambda_x = -0.0094$, $\lambda_y = -0.0458$ and $\lambda_z = -0.6148$ taken at the time $t = 310$. To illustrate this let us take 25 initial conditions distributed over the sphere of radius $r = 0.1$ centered at the point $(1.5, -0.39, 0)$ as it is shown in Figure 6 (a) where it is noticeable that there is a different behavior from the strange attractor of the system without smoothed. Then the radius is reduced to a value of $r = 0.001$, revealing the limit cycle as shows Figure 6 (b). In addition, there are points that are approximately fixed since numerically they are values close to zero.

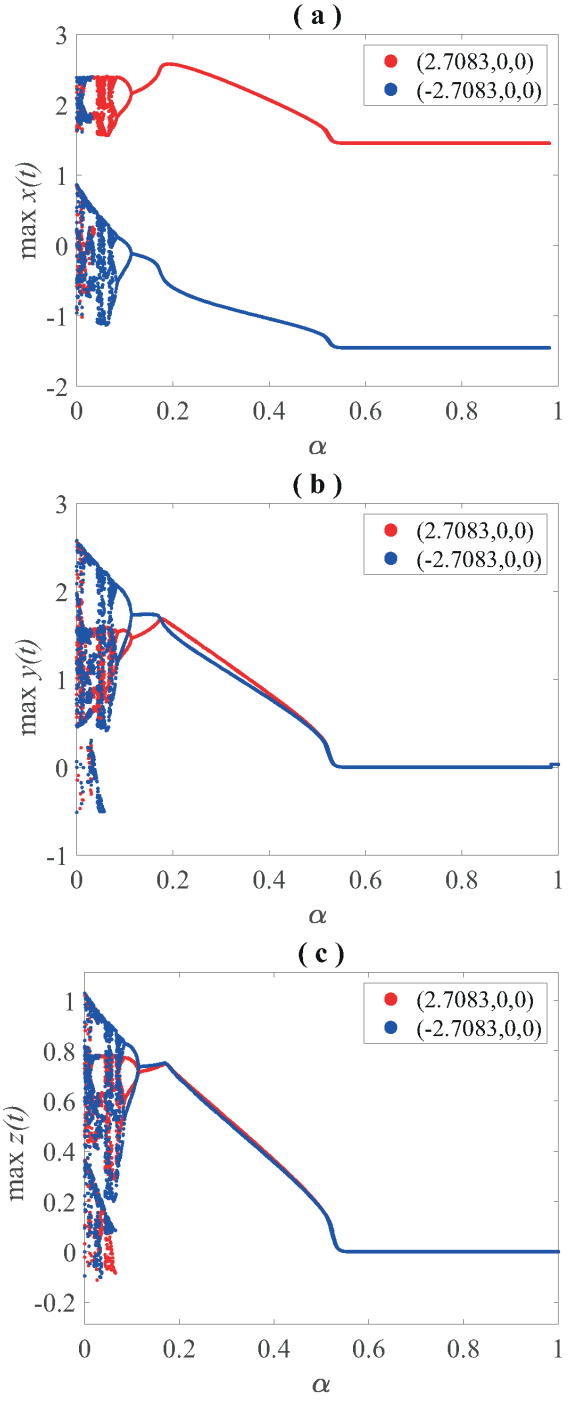

Figure 5 Bifurcation diagrams for the α parameter for the three signals with different initial conditions shown in red and in blue. In the vertical axis it is shown the maxima of corresponding variable.

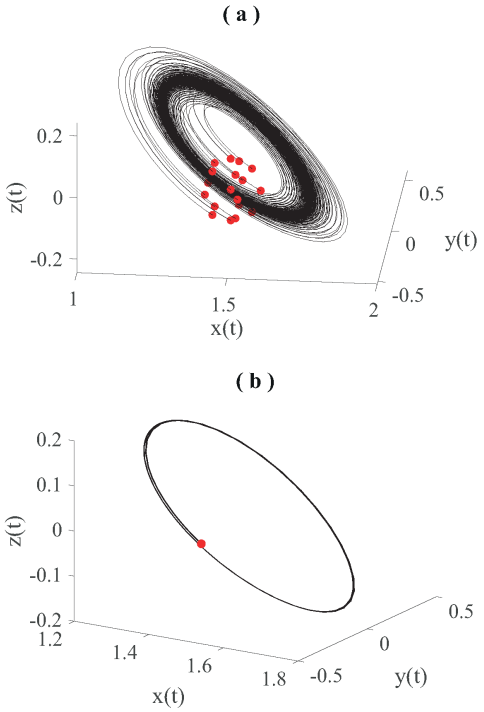

Figure 6 Trajectories in the phase space for smoothed system in Eq. (17) with $\alpha = 0.5$ for initial conditions distributed over the sphere (in red) centered in the point point $(1.5, -0.39, 0)$ with radius $r = 0.1$ in (a) and $r = 0.001$ in (b).

CONCLUSION

Let us briefly discuss the dynamics of the system around the fixed points. Under the values of the parameters c_i, with $i = 1, 2, ..., 5$ previously given, the eigenvalues are found given by the roots of Eq. (9), were it is substituted the function $\mu(x) \to \mu_\alpha(x)$ by using Eq. (18). The eigenvalues are show in Figure 7. According to the classification of the dynamics around fixed points in $3D$ (Francomano *et al.* 2017; Stumpf *et al.* 2011) for the case $\alpha = 0$ (where the distribution of eigenvalues in the complex plane for the different fixed points is shown in Figure 7 (a)), the dynamics are (see Table 1):

$$
\begin{aligned}
(0,0,0) &\quad : \text{Attracting Focus-Saddle.} \\
(p^+,0,0) &\quad : \text{Attracting Focus-Saddle.} \\
(p^-,0,0) &\quad : \text{Repelling Focus-Saddle.} \\
(-p^+,0,0) &\quad : \text{Attracting Focus-Saddle.} \\
(-p^-,0,0) &\quad : \text{Repelling Focus-Saddle.}
\end{aligned}
$$

Note that the dynamics around points $(p^\pm,0,0)$ and $(-p^\pm,0,0)$ is the same. The different types of dynamics are maintained for the values of α shown in Figure 7 (a)-(d) where the imaginary and real parts of the eigenvalues change but remain positive or negative regardless the value of α. Then in (e) of the same figure, the dynamics of the fixed points change to:

$$
\begin{aligned}
(0,0,0) &: \text{Attracting Focus-Saddle.} \\
(p^+,0,0) &: \text{Attracting Focus-Saddle.} \\
(p^-,0,0) &: \text{Asymptotically Stable Focus-Node .} \\
(-p^+,0,0) &: \text{Attracting Focus-Saddle.} \\
(-p^-,0,0) &: \text{Asymptotically Stable Focus-Node .}
\end{aligned}
$$

The results of Figure 7 (f) show that as the value of α increases, the dynamics of the system tend to be only two different types, since the eigenvalues tend to degenerate. Taking a value of $\alpha = 3$ is enough to appreciate this behavior.

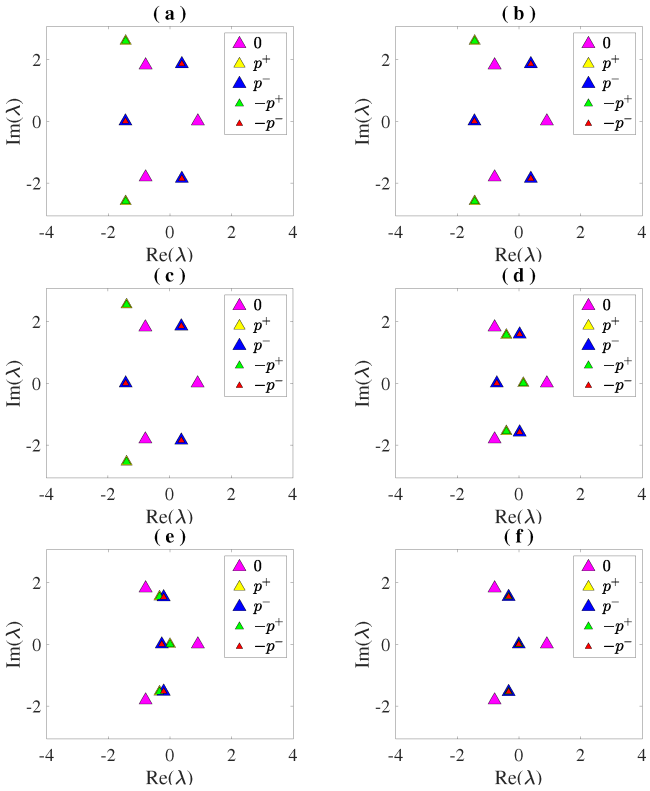

Figure 7 Complex mapping of the eigenvalues λ of the Jerk system for: $\alpha = 0$ (a), $\alpha = 1 \times 10^{-4}$ (b), $\alpha = 1 \times 10^{-2}$ (c), $\alpha = 0.5$ (d), $\alpha = 1$ (e) and $\alpha = 3$ (f). Notice the some eigenvalues coincide for certain values of α, for example for the fixed points p^+ (in yellow) and $-p^+$ (in green).

In this work, a chaotic system, constructed by immersing the Duffing oscillator with a potential type ϕ^6 in a Jerk type system and then adding an exponential smoothed factor to the Duffing potential with a parameter α, that modulates the amplitude of the potential was studied. It was found that for $\alpha = 0$ and for adequate values of the potential there exists a strange attractor, result that was corroborated by using bifurcation diagrams and by analyzing the Lyapunov exponents. By increasing from zero to certain values of α there is found a transition from the chaotic motion to regular one. In some cases the regular motion corresponds to limit cycles.

The way of controlling chaos by means of the function used in this work can also be used in other dynamical system of low- or high-dimensionality.

Expanding upon the current study, future research initiatives may explore other alternative methods for analyzing the dynamics of systems such as the behavior of Lyapunov Exponents as a function of parameters, Poincaré sections, basins of attraction, and exploring different approaches for parameter estimation that induce chaotic behavior in the system. The thorough study of Jerk-type systems with Duffing potential, whose dynamics can transit from periodic to chaotic, provides the opportunity to analyze this behavior in the synchronization of the dynamics of the system to a better understanding on implications and applications of implementing Jerk systems (Uriostegui-Legorreta and Tututi-Hernández

2022; Uriostegui and Tututi 2023; Vaidyanathan *et al.* 2017).

Acknowledgments

This work was supported by Universidad Michoacana de San Nicolás de Hidalgo (UMSNH) and Consejo Nacional de Humanidades Ciencias y Tecnologías (CONAHCYT).

Availability of data and material

Not applicable.

Conflicts of interest

The authors declare that there is no conflict of interest regarding the publication of this paper.

Ethical standard

The authors have no relevant financial or non-financial interests to disclose.

LITERATURE CITED

Chen, D. and Y. Zhang, 2016 Minimum jerk norm scheme applied to obstacle avoidance of redundant robot arm with jerk bounded and feedback control. IET Control Theory & Applications **10**: 1896–1903.

Folifack Signing, V., T. Fozin Fonzin, and M. Kountchou, 2021 Chaotic jerk system with hump structure for text and image encryption using dna coding. Circuits, Systems, and Signal Processing **40**: 4370–4406.

Francomano, E., F. M. Hilker, M. Paliaga, and E. Venturino, 2017 An efficient method to reconstruct invariant manifolds of saddle points. Dolomites Research Notes on Approximation **10**.

Haluszczynski, A. and C. Räth, 2021 Controlling nonlinear dynamical systems into arbitrary states using machine learning. Scientific reports **11**: 12991.

Hilborn, R. C. *et al.*, 2000 *Chaos and nonlinear dynamics: an introduction for scientists and engineers*. Oxford University Press on Demand.

Hong, L., J. Jiang, and J.-Q. Sun, 2015 Fuzzy responses and bifurcations of a forced duffing oscillator with a triple-well potential. International Journal of Bifurcation and Chaos **25**: 1550005.

Kengne, L. K., H. K. Tagne, J. M. Pone, and J. Kengne, 2020 Dynamics, control and symmetry-breaking aspects of a new chaotic jerk system and its circuit implementation. The European Physical Journal Plus **135**: 340.

Louodop, P., M. Kountchou, H. Fotsin, and S. Bowong, 2014 Practical finite-time synchronization of jerk systems: theory and experiment. Nonlinear Dynamics **78**: 597–607.

Louodop, P., S. Saha, R. Tchitnga, P. Muruganandam, S. K. Dana, *et al.*, 2017 Coherent motion of chaotic attractors. Physical Review E **96**: 042210.

Natiq, H., S. Banerjee, and M. Said, 2019 Cosine chaotification technique to enhance chaos and complexity of discrete systems. The European Physical Journal Special Topics **228**: 185–194.

Njitacke, Z. T., C. Feudjio, V. F. Signing, B. N. Koumetio, N. Tsafack, *et al.*, 2022 Circuit and microcontroller validation of the extreme multistable dynamics of a memristive jerk system: application to image encryption. The European Physical Journal Plus **137**: 619.

Patidar, V. and K. Sud, 2005 Bifurcation and chaos in simple jerk dynamical systems. Pramana **64**: 75–93.

Posch, H. A., W. G. Hoover, and F. J. Vesely, 1986 Canonical dynamics of the nosé oscillator: Stability, order, and chaos. Physical review A **33**: 4253.

Raineri, M. and C. G. L. Bianco, 2019 Jerk limited planner for real-time applications requiring variable velocity bounds. In *2019 IEEE 15th International Conference on Automation Science and Engineering (CASE)*, pp. 1611–1617, IEEE.

Sandri, M., 1996 Numerical calculation of lyapunov exponents. Mathematica Journal **6**: 78–84.

Sharker, S. I., S. Holekamp, M. M. Mansoor, F. E. Fish, and T. T. Truscott, 2019 Water entry impact dynamics of diving birds. Bioinspiration & biomimetics **14**: 056013.

Sprott, J. C., 2011 A new chaotic jerk circuit. IEEE Transactions on Circuits and Systems II: Express Briefs **58**: 240–243.

Stumpf, P. P., Z. Sütő, and I. Nagy, 2011 Research in nonlinear dynamics triggered by r&d experiences .

Uriostegui, U. and E. S. Tututi, 2023 Master-slave synchronization in the van der Pol and duffing systems via elastic, dissipative and a combination of both couplings. Journal of Applied Research and Technology **21**: 227–240.

Uriostegui-Legorreta, U. and E. Tututi, 2023a Control and synchronization in the Duffing-van der Pol and Φ^6 duffing oscillators. Indian Journal of Physics pp. 1–13.

Uriostegui-Legorreta, U. and E. S. Tututi, 2023b Master-slave synchronization in the Duffing-van der Pol and Φ^6 duffing oscillators. International Journal of Nonlinear Sciences and Numerical Simulation **24**: 1059–1072.

Uriostegui-Legorreta, U. and E. S. Tututi-Hernández, 2022 Master-slave synchronization in the rayleigh and duffing oscillators via elastic and dissipative couplings. Revista de ciencias tecnológicas **5**.

Vaidyanathan, S., A. Sambas, M. Mamat, and M. S. WS, 2017 Analysis, synchronisation and circuit implementation of a novel jerk chaotic system and its application for voice encryption. International Journal of Modelling, Identification and Control **28**: 153–166.

Wolf, A., J. B. Swift, H. L. Swinney, and J. A. Vastano, 1985 Determining lyapunov exponents from a time series. Physica D: nonlinear phenomena **16**: 285–317.

Zhang, H., D. Liu, and Z. Wang, 2009 Chaotification of nonchaotic systems. Controlling Chaos: Suppression, Synchronization and Chaotification pp. 309–341.

Zhou, J., D. Xu, and Y. Li, 2010 Chaotifing duffing-type system with large parameter range based on optimal time-delay feedback control. In *2010 International workshop on chaos-fractal theories and applications*, pp. 121–126, IEEE.

How to cite this article: Bucio-Gutiérrez, A., Tututi-Hernández, E. S., and Uriostegui-Legorreta, U. Analysis of the Dynamics of a ϕ^6 Duffing Type Jerk System. *Chaos Theory and Applications*, 6(2), 83-89, 2024.